BORON-INCORPORATED DIAMOND TO ACT AS ELECTRODE MATERIAL IN LITHIUM ION BATTERIES

M. ULLAH[a*], A. M. RANA[b], E. AHMED[b], R. RAZA[c], Z. A. SHAH[a], ENGR. M. AHMAD[d]
[a]*Department of Physics, Government College University Faisalabad, Layyah Campus Layyah, Pakistan*
[b]*Department of Physics, Bahauddin Zakariya University, Multan-60800, Pakistan*
[c]COMSATS Institute of Information Technology, Defence Road, Off Raiwind Road, Lahore 54000, Pakistan
[d]*QEC, Government College University Faisalabad, Layyah Campus Layyah, Pakistan*

A crystalline electrode made up of 75% active material (boron-incorporated diamond, BID), 10% poly vinylidene fluoride + 1-methyl-2pyrrolidinone and 15% carbon black was synthesized using the combustion technique at 1173 K for one hour to make homogeneous distribution of sub-micron sized particles. Characterization of the electrode material has been performed through X-ray diffraction, Raman Spectroscopy and Scanning electron microscopy before using it in lithium-ion batteries. The amount of Li in the boron-doped diamond strongly affects its electrochemical performance as electrode. Electrochemical measurements have illustrated much better cycling stability in the –4.0 to 4.5V range at different rates of current. The successful electrochemical activity of boron-incorporated diamond electrode along with lithium electrode insertion in Li^+ ion batteries has been reported and discussed here. The peak current shows an almost linear relationship with square root of the scan rate. In addition, effective electrode area was estimated to be 0.54 cm^2.Electronic properties of Li-containing electrodes were investigated using DFT approach which showed polaronic conducting behavior which seems advantageous for high power capability.

(Received April 11, 2017; Accepted July 18, 2017)

Keywords: Boron-incorporated diamond electrode, Lithium-ion batteries, Layered cathode, Electrochemical cycling and cyclic voltammetry.

1. Introduction

Now-a-days lithium ion batteries have a lot of commercial applications as these batteries possess very good capacity for storage of energy with very low memory effects and long lifetime when compared with other types of batteries [1].Most commonly used cathode materials in these batteries are transition metal oxides including $LiMn_2O_4$ [2], $LiCoO_2$ [3,4], $LiNiO_2$etc. [5, 6]. $LiMn_2O_4$ is found to be economical and less pollutant to the environment; however it demonstrates poor cycling performance. The diffusivity of $LiCoO_2$ is high, but it becomes expensive when large amount of Co is used [3,4]. $LiNiO_2$ is also a potential material for cathodes but stoichiometric$LiNiO_2$ is difficult to make and its thermal stability is low as it is charged [7]. The operation of electrodes inside lithium-ion batteries depends on the processes of intercalation, which involves the exchange of Li^+ ions with much open lattice structure. The success of intercalation electrodes is due to their small structure, faster diffusion rate of Li^+ ions and changes in volume. Such intercalation anodes are based onsp^2-linked carbon (e.g. graphite, coke etc.) and are in common use because they have good chemical stability and low cost. The only disadvantage of these electrodes is that they demonstrate much limited capacity of charge storage that's why

*Corresponding author: mahtabullah@yahoo.com

they are not much successful in fulfilling the needs of higher energy, long lifetime and power density usage in practical applications. To address such shortcomings, several other materials have been investigated. Diamond has been recognized as the most potential material for such applications. Being electrically insulating, un-doped diamond is not beneficial for its applications as a material to make electrodes. However, diamond can behave like conducting materials when it is doped with some definite elements as other large band gap materials can do. Presently, p-type semiconducting diamonds are being produced using mostly boron as dopant. Such boron-incorporated diamond (BID) electrodes are found to be smart materials for Li^+ ion batteries as they improve stability of lithium ions by boron defects [8, 9]. Yuan et al. [10] examined the electronic structure and vibration spectroscopy of *graphite*-BC_3 theoretically and described strong localization of electron-density between carbon atoms in the hexagonal rings involving only C atoms. This fact suggests that C−C bonds are much stronger as compared to B−C bonds. But these weaker B−C bonds are capable of retaining hexagonal symmetry in the structure of *graphite*-BC_3, consequently carbon hexagons preserve weak bonding. Since boron possesses lower valence as compared to that of carbon, so *graphite*-BC_3 structure becomes an electron deficient than simple graphite, and this makes it relatively less stable. When lithium is doped, *s* electrons from Li atoms are donated to the π-system of such electron-deficient structure, providing more stability of the structure. Therefore, maximum Li content present in the *graphite*-BC_3structureshould be greater than that normally found in the most intercalated graphite (LiC_6). In addition, transfer of electrons from Li atoms to adjacent B atoms occurs at a larger rate which may become a cause of the broader distribution of electrostatic potential as compared to LiC_6, consequently potential barrier for the diffusion of Li^+ ions decreases. It hopefully contributes to the migration of Li^+ ions and hence improves the performance of battery. Another advantage of the BID electrodes is that they have ability of changing their surface properties in a quicker way, which makes them useful for wider variety of applications including electro-synthesis, electro-analysis and electro chemically remediation of toxic waste [10].

In this present paper, we report the fabrication and characterization of the BID electrode to understand its structural variations and an insight into its electrochemical behavior when it is playing the role of a cathode in lithium-ion batteries.

2. Experimental

Boron-incorporated polycrystalline diamond films of 4 microns thickness have been coated on Si wafers acting as substrates inside the chamber of a hot-filament chemical vapor deposition (HFCVD) apparatus. The chamber was filled with a mixture of methane and hydrogen and boron-carbide blocks were placed in the vicinity of tungsten filaments for the incorporation of boron into diamond. After deposition, chemical etching of Si wafer was performed to get a free-standing diamond layer. This diamond layer was laterally laser-cut into pieces of 3 to 5 μm size. Aluminum foil was used to form positive electrodes by dispersing a mixture that contains 75% boron-incorporated diamond + 10% poly vinylidene fluoride + 15% carbon black and 1-methyl-2pyrro-lidinone over it. These electrodes (Circular in shape with an area of~3 cm^2) were then dehydrated inside the argon-filled glove box (<3 ppm H_2O and O_2) at ~ 400 K before assembling the cell. The cell was fabricated that contains positive (BID) and negative (Li foil) electrodes separated through glass-wool soaked in an electrolyte, which composed of 1M $LiPF_6$ (lithium hexafluorophosphate) liquefied in a solution of ethylene carbonate and diethyl carbonate (with volume ratio of 2:1).The cell was then vacuum-packed inside an Al foil coated with a polymer, the nickel and aluminum contacts were also attached for measurements. The galvanostatic cycles were performed on these cells through a battery testing system (Digatron BTS 600).

Characterization of the electrode materials was done through scanning electron microscopy (SEM) using HR-SEM LEO 1550 and Raman spectroscopy before any electrochemical investigations. The back scattering geometry was applied to record Raman spectra at room temperature using Renishaw 2000 micro-Raman system with visible excitation.

Cyclic Voltammetry (CV) was performed to study the electrochemical response of the electrode device using Eco Cherie Autolab PGSTAT 302 potentiostat/galvanostat (Netherlands,

with GPES 4.9software) in a three electrode configuration. As counter electrode a platinum rod was utilized whereas Ag/AgCl(0.1 M KCl) served the role of reference electrode. Deoxygenation of all the solutions was made in N_2atmosphere for a minimum time interval of 15 min before any measurements and throughout the experiment deionized water was used.

3. Results and discussion

3.1 Raman spectrum and SEM analyses

Fig. 1(a) illustrates typical Raman spectrum of BID electrode containing diamond grains along with graphite-like phase. The spectrum contains sharp peak at the frequency of 1333cm^{-1}. This sharp peak corresponds to sp^3 hybridized carbon. The shifting of characteristic diamond vibration at 1332 cm^{-1} to a frequency of 1333 cm^{-1}may be caused by the interaction of Raman photons with the imperfections induced by the doping of Li + carbon + boron resulting in the decrease of photon energy. Moreover, there may be internal stresses present in Li + carbon + boron sheets and compressive stresses are capable of shifting diamond peak [11]. A broad peak(hump)observed around wave numbers of 1510−1560 $cm^{-1}$is the characteristic of graphitic phase. This hump originates because of the bond stretching of all pairs of sp^2locationsand termed as G peak [12].

SEM image of the particularly selected sample of boron-diamond electrode is shown in Fig. 1(b). It is noted that the electrode contains randomly distributed small and large particles of different shape and size ranging from 0.4 to 0.6 μm.

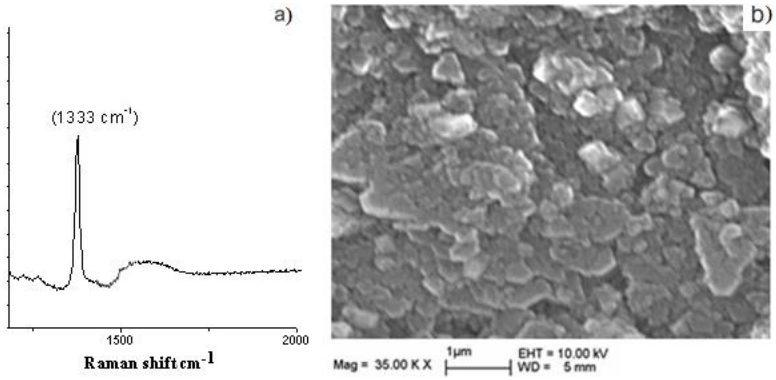

Fig.1.a) Raman spectrum, and b)Scanning electron micrograph of boron-doped diamond electrode.

3.2 Electrochemical lithium extraction and Structural variations

For the investigations of any structural variations occurring in the boron-diamond electrode as Li^+-ion extraction takes place electrochemically, a comprehensive study on X-ray diffraction of Li-carbon-boron system for various values of Li content was performed. The charging curve for the first cycle at some chosen composition of Li in the cell (for *ex-situ* XRD measurements)and the charge-discharge test of the battery are shown in Fig. 2(a) and 2(b) respectively. The expanded view of XRD patterns of the BID samples with different Li content are illustrated in Fig. 3. Such expanded view of XRD patterns in the 2θ range from 38-48°provides information regarding the development of cubic unit-cell variables. XRD results indicate no phase change occurring due to lithium extraction. Furthermore, the {111}reflection observed at 2θ~42°has been shifted to higher angles during charging with increasing amount of Li content. This peak shift could be attributed to electrostatic repulsion that increases across the van der Waals cavity between the Li-carbon-boron sheets[13].

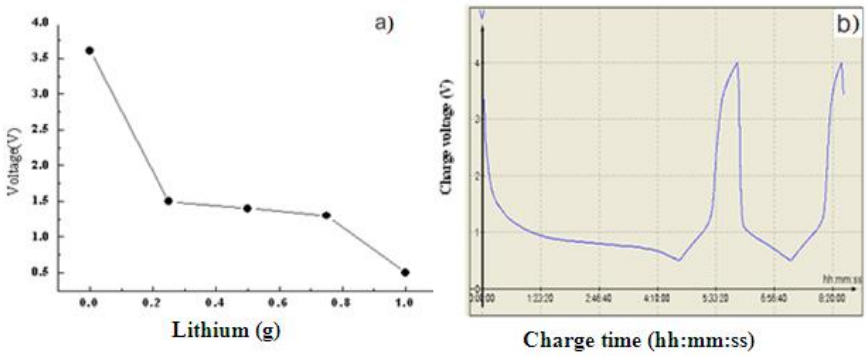

Fig. 2. a) Voltage profile and b) Battery test: charge-discharge cycles of the boron-incorporated diamond electrode.

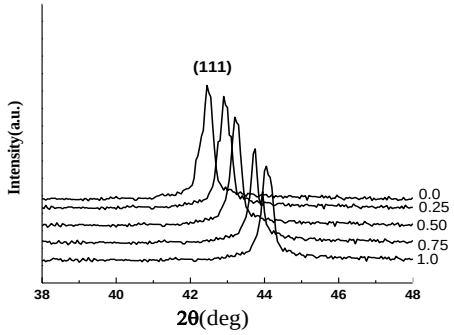

Fig.3.X-ray diffraction patterns for boron-doped diamond electrode as a function of lithium amount as indicated against each diffraction pattern.

The penetration of lithium atoms into graphite plates occurs during intercalation in graphite. During this process, Li atoms become Li^+ cations by partial donation of their *s* electrons to graphite plates. The Li-Li ionic repulsion suppresses the maximum content of Li between neighboring graphite plates yielding LiC_6in which the mass fraction of Li is 8.7% [14-16]. As lithium content in BID electrode goes on rising, this Li-Li ionic repulsion surpasses the attractive energy related to the lithium-carbon bonds. This leads to the thermodynamic instability of the structure.

3.3 Cyclic voltammetry characteristics

To examine the nature of electro active species, cyclic voltammetry is the commonly used electro analytical method. It can be utilized to evaluate the electrode surfaces electrochemically. The most common use of this technique is to determine the electrochemical characteristics of an electrode material with the help of aqueous solution of ferric/ferricyanides [17].

Fig. 4shows the cyclic voltammogram observed on BID electrode inside the 0.1MKCl at scanning speed of 1 V/s. One can see much wider potential window showing low background current. The voltammograms presented in Fig. 5(a) have been noted in 0.1MKCl+ 1M $K_3Fe(CN)_6$ solution at different scan rates. It is clearly seen from Fig. 5(a) that these graphs depict a symmetric peaks related with anodic and cathodic behavior, which may be attributed to the reduction and oxidation of ferricyanide-ferrocyanidepairat the interface between boron-incorporated diamond and the solution. The peak separation of the cathodic and anodic features denoted by ΔE_p is an obvious indication of the degree of irreversibility in electrochemical reaction occurring at various scan rates.

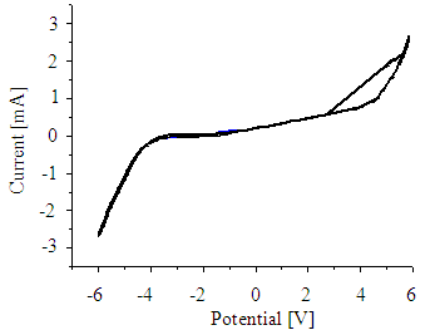

Fig.4. Cyclic voltammetric 'CV' plot of boron-incorporated diamond electrode in a solution of 0.1M KCl at the scan speed of 1 V/s.

As boron-incorporated diamond (active material) involves the addition of Li, there appears an oxidative wave at ~ −0.5 V. Furthermore, it is noticed that there is a rise in the peak height with increasing the content of boron-incorporated diamond and Li (Fig. 5).Such behavior of the curves can be associated with the oxidation of boron-incorporated diamond + Li. Moreover, such electrochemical characteristics look basically the same as observed for the diamond electrodes with1, 4-difluorobenzene.

It is clear from Fig. 5(a) that the least value of ΔE_p observed during measurement is 0.50 V at a range from -0.2 to 0.6V. The ΔE_p has increased as the scan rate increased and this rise might be related with slow reaction of transfer of electron at the interface between boron-incorporated diamond electrode and the solution. It is speculated that higher electrical resistivity of diamond can be a cause of such higher values of ΔE_p[18, 19]. The highest observed value of ΔE_p is 2.05 V at a range from -0.2 to 0.1V. This could be caused by a large transfer of electrons from Li atoms to nearby boron one's. This electron transfer relatively leads to a broader distribution of electrostatic potential and hence results in a decrease of potential barrier to the movement of Li^+ ions. This may improve the migration of Li^+ ions. In addition, the transfer of *s* electrons from Li atoms takes place towards the π-system of a structure deficient in electrons; this improves the stability of structure [10]. Thus the stabilization of lithium by boron defects takes place. Electrochemical variables related to diamond electrodes were determined from voltammograms depicted in Fig. 5(a) and are presented in Table 1.Thepeak ratio (I_{pa}/I_{pc}) between anodic and cathodic currents is not uniform except for that obtained at scan rate of 5 V/s. This shows that a quasi-reversible redox reaction of $K_3Fe(CN)_6$ has occurred on this electrode. Moreover, the reaction will be more irreversible if ΔE_p becomes higher [20, 21]. This leads to the occurrence of a quasi-reversible reaction (Fig. 5(a)) which can be expected in the case of diamond electrodes [22, 23].

In order to estimate the effective area of these BID electrodes, a graph between the peak current at anode and square root of the scan rate (v) can be drawn as illustrated in Fig. 5(b). The slope of this plot can be used to determine the operative area of BID electrodes in accordance with the relation by Randles-Sevcik [24]:

$$I_p=2.69x10^5 n^{3/2} D_o^{½} v^{½} A C_o \quad (1)$$

In this relation I_p stands for peak current, n = 1 denotes the stoichiometry of electrons, A is the effective area (cm^2) of the electrode, C_o indicates concentration in the bulk (1 M($mole/cm^3$)), D_o gives the diffusion coefficient ($1.52x10^{-5}$ cm^2/s) for $K_3Fe(CN)_6$ [25]and constant has units $C/(mole\text{-}V^{1/2})$. As expected from equation (1), I_p should increase linearly with $v^{0.5}$ as shown in Fig. 5(b).This plot depicts almost linear behavior. Using slope of this plot, the effective area of the BID electrode was estimated to be 0.054 cm^2.

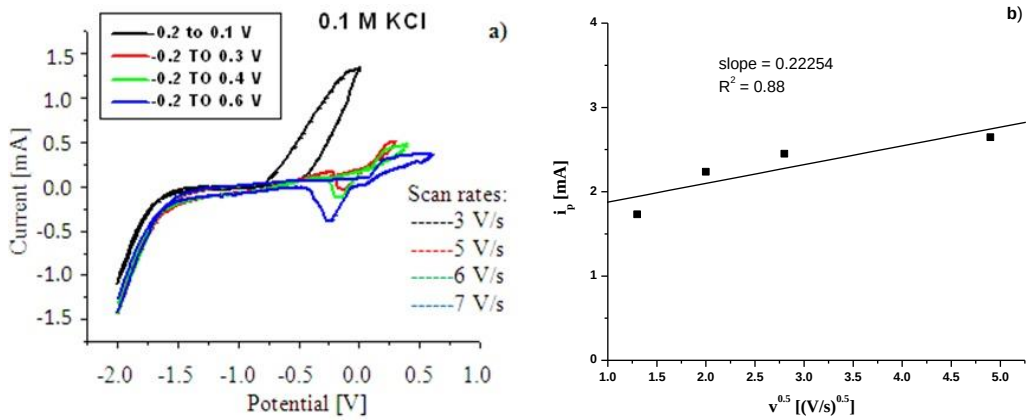

Fig.5.a) Cyclic voltammograms 'CVs' recorded for boron-incorporated diamond electrodes in a 0.1M KCl+ 1M $K_3Fe(CN)_6$ at the scan rates of v = 3, 5, 6, 7 (V/s); b) Peak current i_p vs. square root of the scan rate ($v^{0.5}$).

3.4 Electronic properties

Vienna ab-initio simulation package (VASP) was applied for theoretical calculations of electronic charge density within the framework of plane-wave density functional theory (DFT) [26, 27]. Regarding these calculations, Perdew−Burke−Ernzerhof functionals, generalized gradient approximation and projector augmented wave technique were considered to represent interactions between ions, electrons and electron interchange effects [28–30]. Fig.6 shows the partial (a) and total (b) density of states (DOS) of Li-containing boron-doped diamond films. Li 1s states in the valence band just touch the Fermi level. Moreover, it is obvious from this figure that Li 1s states play dominant role in the conduction as well as valence bands. However, Li 2s states are dominant in the energy range from ~ -12 eV to ~ -22 eV. In addition a band gap of 4.6 eV is obvious from total density of states (TDOS) plot (see Fig. 6(b)). The above said facts illustrate the polaronic conductor's behavior analogous to that observed in olivine phosphates as studied by Seo et al.[26]. In addition, the presence of Li defects in boron doped diamond films may be advantageous for high power capability.

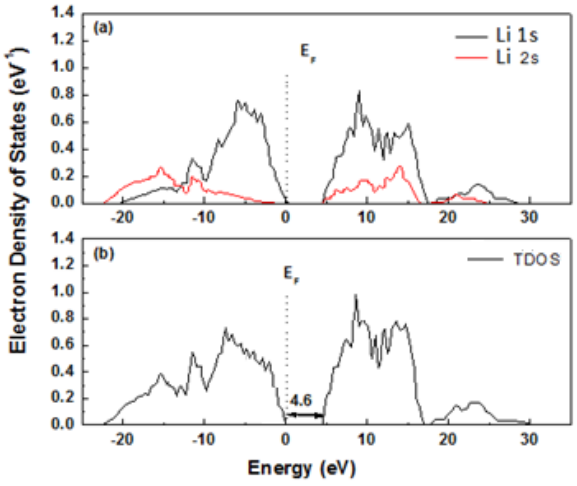

Fig. 6: Partial and total DOS of Li-containing cathode material (boron-incorporated diamond) showing occupied and unoccupied bands. E_F represents the Fermi level.

Table1. List of the data determined from CV plots depicted in Fig. 5.

Scan rate (V/s)	E_{pa} (V)	E_{pc} (V)	ΔE_p (V)	I_{pa} (mA)	I_{pc} (mA)	I_{pa}/I_{pc}
3	-0.80	1.25	2.05	0.15	1.25	0.12
5	-0.29	0.29	0.56	0.20	0.20	1.00
6	-0.28	0.27	0.54	0.25	0.50	0.50
7	-0.25	0.25	0.50	0.40	0.51	0.78

4. Conclusions

BID electrode has been fabricated through combustion technique and examined to behave as positive electrode for their possible applications in Li^+ ion batteries. SEM and Raman spectroscopic analyses confirm that the present boron-incorporated diamond electrode also contains some graphite-like phase, which is very good for stabilization of lithium atoms. Present results illustrate that electrochemical performance of the cathode material depends on structural morphology as well as on the distribution of cations in the crystal lattice. Both of these factors are linked to the fabrication conditions. XRD data confirms ordered layered structure of boron-incorporated diamond electrode that resulted in the best electrochemical performance.

The cyclic voltammetry data demonstrated the electrochemical stability of BID electrodes in aqueous solution of KCl for voltage ranging from−4.0 V to +4.5 V for their possible uses in Li^+-ion batteries. Lithium atoms inside the structure move more freely at a range from -4.0 to 4.5V. The higher values of cathodic and anodic peak separation ΔE_p(>2.05V)can be attributed to quasi reversible character of the electrochemical reaction taking place on the surface of BID electrode. The rise of peak separation current I_p occurs with raising the scan rate. The ratio of currents (I_{pa}/I_{pc}) varies with scan rate. Moreover, current ratio is almost unity at scan rate of 5 V/s. This electrochemical behavior is caused by high electrical resistivity of BID electrode. Using Randles-Sevcik equation, the effective area of the BID electrode was estimated to be 0.054cm^2. Electronic properties of Li-doped electrode showed polaronic conductors behavior similar to olivine phosphates and advantageous for high power capability.

Acknowledgement

Authors acknowledge the financial support of Higher Education Commission (HEC), Pakistan under International Research Support Initiative Program (IRSIP). Authors also thank to Dr. Hanif Mirrani for technical correction of chemicals names and their formulas.

References

[1] A.R. Armstrong, P.G. Bruce, Letter Nature**381**, 499 (1996).
[2] K. Mittzushima, P.C. Jones, P.J. Wiseman, J.B. Goodenough, Materials Research Bulletin **15**, 783(1980).
[3] J.R. Dahn, U. von Sacken, C.A. Michal, Solid State Ionics **44**, 265 (1990).
[4] K. Ozawa, Solid State Ionics **69**, 212 (1994).
[5] C. Delmas,M.Me´ne´ trier, L. Croguennec, I. Saadoune, A. Rougier, C. Pouillerie, G.Prado, M. Gru¨ne, L. Fourne`s, ElectrochimicaActa**45**, 243 (1999).
[6] T. Ohzuku, A. Ueda, Solid State Ionics **69**, 201 (1994).
[7] Y. Nishida, K. Nakane, T. Stho, Journal of Power Sources **68**, 215 (1998).
[8] C. B. Qiang Xu, A. C. Dillon, S.-H. Wei, and Y. Zhao, Journal of Physical Chemistry Letters

2, 1129(2011).
[9] E. Lowther, P. V. Zinin, and L. C.Ming, Physical Review B **79**, 33401(2009).
[10] Yuan Yu, Yanli Zhou, LiangzhuanWu, JinfangZhi, International Journal of Electrochemistry **2012**, 567171 (2012).
[11]G.Gouadec, P.Colomban, Progress in Crystal Growth and Characterization of Materials, **xx**, 1 (2007).
[12] Y.-Q. Fu, C.-Q.Sun, H.-J.Du, B.-B. Yan, Journal of Physics D: Applied Physics**34**, 1430 (2001).
[13] M. Dahbi, J. Magnus Wikberg, I. Saadoune, T. Gustafsson, P.Svedlindh, K.Edström,ElectrochimicaActa**54**, 3211 (2009).
[14] D. Bandyopadhyay, European Physical Journal D**54,** 643 (2009).
[15] K. R. Kganyago, P. E. Ngoepe, Physical Review B **68**, 205111(2003).
[16] J. R. Dahn, Physical Review B **44,** 9170 (1991).
[17] R. Torz-Piotrowska, A. Wrzyszczyñski, K. Paprocki,M. Szreiber, C. Uniszkiewicz,E. Staryga, Journal of Achievements in Materials and Manufacturing **37**, 486 (2009).
[18] R. Ramesham, M.F. Rose, Diamond Related Materials**6**, 17 (1997).
[19] R. Ramesham, M.F. Rose, Thin Solid Films **300**, 144 (1997).
[20] Y.V. Pleskov, M.D. Krotowa, V.I. Polyakov, A.V. Khomich, A.J. Rukovischuikov, B.L. Druz, I. Zaritsky, Journal of Electroanalytical Chemistry **519**, 60 (2002).
[21] A.J. Bard, L.R. Faulkner, Electrochimica Methods: Fundamentals and Applications, Wiley,1980 (Chapter 3).
[22] N.G. Ferreira, L.L.G. Silva, E.J. Corat, V.J. Trava – Airoldi, Diamond and Related Materials **11**, 1523 (2002).
[23] V. Fischer, D. Gaudini, S. Laufer, E. Blauk, Ch. Comminelis, ElectrochimicaActa**44**, 521 (1988).
[24]Y.V. Pleskov, A.Y. Sakharova, M.D. Krotova, L.L. Bouilov, B.P. Spitsyn, Journal of Electro analytical Chemistry **228**, 19 (1987).
[25] G.Perenlei, T.Wee Tee, N.AzahYusof, G. JooKheng, International Journal ofElectrochemicalScience**6**, 520(2011).
[26] D. H. Seo, Y. U. Park, S. W. Kim, I. Park, R. A. Shakoor, K. Kang, Physical Review B: Condensed Matter Physics **83**, 205127 (2011).
[27] G. Kresse, J. Furthmuller, Computational Materials Science**6**, 15(1996).
[28] J. P. Perdew, K. Burke, M. Ernzerhof, Physical Review Letters**77**, 3865 (1997).
[29] P. E. Blochl,Physical Review B: Condensed Matterand Materials Physics**50**, 17953 (1994).
[30] G. Kresse, D. Joubert, Physical Review B: Condensed Matter and Materials Physics**59**, 1758 (1999).